HHS Public Access

Author manuscript

Mol Microbiol. Author manuscript; available in PMC 2021 January 01.

Published in final edited form as:

Mol Microbiol. 2020 January ; 113(1): 285–296. doi:10.1111/mmi.14416.

Changes in transcription start sites of Zap1-regulated genes during zinc deficiency: Implications for *HNT1* gene regulation

Supinda Tatip[1,2], **Janet Taggart**[2], **Yirong Wang**[2], **Colin W. MacDiarmid**[2], **David J. Eide**[2,*]

[1]Department of Biology, Faculty of Science, Mahidol University, Bangkok, Thailand [2]Department of Nutritional Sciences, University of Wisconsin-Madison, Madison, WI, USA

SUMMARY

Changes in RNA are often poor predictors of protein accumulation. One factor disrupting this relationship are changes in transcription start sites. Therefore, we explored how alterations in transcription start site affected expression of genes regulated by the Zap1 transcriptional activator of *Saccharomyces cerevisiae*. Zap1 controls their response to zinc deficiency. Among over 80 known Zap1-regulated genes, several produced long leader transcripts (LLT) in one zinc status condition and short leader transcripts (SLT) in the other. Fusing LLT and SLT transcript leaders to GFP indicated that for five genes, the start site shift likely has little effect on protein synthesis. For four genes, however, the different transcript leaders greatly affected translation. We focused on the *HNT1* gene. Zap1 caused a shift from SLT *HNT1* RNA in zinc-replete cells to LLT *HNT1* RNA in deficient cells. This shift correlated with decreased protein production despite increased RNA. The LLT RNA contains multiple upstream open reading frames that can inhibit translation. Expression of the LLT *HNT1* RNA was dependent on Zap1. However, expression of the long transcript was not required to decrease SLT *HNT1* mRNA. Our results suggest that the Zap1-activated LLT RNA is a "fail-safe" mechanism to ensure decreased Hnt1 protein in zinc deficiency.

Graphical Abstract

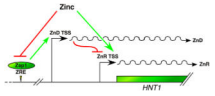

Abbreviated Summary

We show here that Zap1 and zinc deficiency in *Saccharomyces cerevisiae* shifts the *HNT1* transcription start site (TSS) from close to the gene to a more distal location. The longer RNAs produced in zinc-deficient cells contain upstream open reading frames that repress their translation. Moreover, these longer RNAs also repress the proximal *HNT1* promoter and complement other regulatory factors by serving as a "fail-safe" or override switch to ensure low expression during zinc deficiency.

*Corresponding author: deide@wisc.edu, 608-263-1613, 1415 Linden Drive, Madison, WI 53706.

Keywords

Saccharomyces cerevisiae; zinc; regulation; transcription factors; promoter regions; RNA; transcription start site

INTRODUCTION

In many studies, changes in mRNA levels in response to some stimulus are assumed to cause corresponding changes in protein levels. While this correlation is often confirmed by subsequent studies, there is an increasing number of genes where changes in transcript level do not reflect changes in protein abundance (Vogel and Marcotte, 2012). This disconnect between mRNA and protein levels may be due to several factors including translational control, altered splicing, or changing rates of protein degradation. Another key and often unrecognized factor that can influence protein expression are changes in the start site of transcription. The resulting differences in 5' transcript leader sequences can have large effects on translation initiation and/or elongation and, therefore, protein abundance (Arribere and Gilbert, 2013).

We are studying these issues in the yeast *Saccharomyces cerevisiae* with a specific focus on the genes regulated by the Zap1 transcription factor. Zap1 is the central regulator of zinc homeostasis and the adaptive response to zinc deficiency in this yeast. It is a transcriptional activator that turns on transcription in zinc-deficient cells and zinc directly (Eide, 2009) and perhaps indirectly (Frey et al., 2011) inhibits Zap1 activity in replete cells. Zap1 binds to one or more conserved 11 bp sequences in its target promoters that has the consensus sequence of ACCTTNAAGGT (where N is any base) called a zinc-responsive element or ZRE. Previous studies have led to the identification of over 80 genes in the *S. cerevisiae* genome that are likely to be direct targets of Zap1 regulation (Bird et al., 2006a; De Nicola et al., 2007; Lyons et al., 2000; MacDiarmid et al., 2016; Singh et al., 2017; Taggart et al., 2018; Wu et al., 2008; Wu et al., 2009).

For most Zap1-regulated genes studied to date, Zap1-mediated increases in RNA level result in increased levels of the encoded proteins (Eide, 2009). An exception to this rule is the recently characterized *RTC4* gene, which has increased levels of RNA in zinc-deficient cells and markedly decreased protein levels in those same cells (Taggart et al., 2017). This paradox was resolved when the transcription start sites for *RTC4* were mapped in both zinc-replete and deficient cells. This analysis showed that in zinc-replete cells, *RTC4* is transcribed with a relatively short 5' transcript leader, termed the short leader transcript or SLT, that is efficiently translated. In zinc-deficient cells, Zap1 binds to a ZRE located upstream of the proximal *RTC4* promoter and activates transcription of a long leader transcript (LLT) RNA that represses transcription of the SLT RNA from the proximal promoter due to physical occlusion and/or repressive chromatin modifications recruited to the region by RNA polymerase II transcription. Despite encoding the full *RTC4* open reading frame, Rtc4 protein is not translated from the LLT RNA due to the presence of four upstream open reading frames (uORFs) in the 5' transcript leader that inhibit translation of the Rtc4-encoding ORF.

RTC4 is one example of a gene which shows increased transcription coupled to decreased translation. Because of this example, we examined other members of the Zap1 regulon for related effects and the results of that analysis are reported here. In brief, we found that several Zap1 target genes in addition to *RTC4* show altered sites of transcription initiation when comparing zinc-replete and deficient conditions. Three genes, *RAD27*, *MNT2*, and *HNT1* appeared to follow the paradigm established by *RTC4*. *HNT1* encodes an adenosine monophosphoramidase that was proposed to regulate TFIIH activity (Bieganowski et al., 2002; Korsisaari and Makela, 2000). This gene was of particular interest because it is the yeast ortholog of the *HINT1* gene in humans. Mutations in *HINT1* have been shown to cause axonal, motor-predominant Charcot-Marie-Tooth (CMT) neuropathy, frequently associated with neuromyotonia (Zimon et al., 2012). Intriguingly, mutations in the yeast *HNT1* gene are complemented by expression of a mammalian *HINT1* ortholog indicating a conservation of biological function (Bieganowski et al., 2002). In this report, we focused on regulation of *HNT1* by zinc and the Zap1 transcription factor. Our results indicate that *HNT1* is regulated by a mechanism similar to *RTC4* but, in contrast, they also suggest that this mechanism serves as a "fail-safe" or override switch mechanism that complements other regulators controlling *HNT1* expression.

RESULTS

In a previous study, we mapped transcription start sites across the yeast genome in zinc-replete and deficient cells (Wu et al., 2016). That analysis discovered numerous changes in transcription start sites between these two conditions. Of the ~80 known or likely Zap1-regulated genes, clear shifts in transcription start sites were found for nine genes. These included *RTC4* (Taggart et al., 2017) as well as three other genes, *RAD27*, *HNT1*, and *MNT2* that had longer 5' transcript leaders in zinc-deficient cells than were generated in replete cells (Figure 1). Five other genes, *FET4, MCD4, ZRC1, ZRT3*, and the *ZAP1* gene itself, showed the opposite effect with longer 5' transcript leaders expressed in zinc-replete cells and shorter 5' transcript leaders expressed in deficient cells. For each gene, we designated the longer RNA products as "long leader transcripts" (LLT) and the shorter RNAs as "short leader transcripts" (SLT). No change in transcription start sites were observed for the *CMD1* control gene.

Many of the LLT 5' transcript leaders include uORFs that might inhibit translation of the protein-coding ORF and are absent from the SLT 5' transcript leaders (Figure 2A). In addition, longer 5' transcript leaders may form more stable secondary structures that could also inhibit translation (Pickering and Willis, 2005). Therefore, the observed changes in 5' transcript leader lengths could affect the abundance of proteins encoded by these Zap1-regulated genes aside from changes in total RNA abundance. To test this hypothesis and determine the effect of the different 5' transcript leaders on protein accumulation, we constructed plasmids expressing the most abundant LLT and SLT 5' transcript leaders for each gene (Figure 1) fused to the open reading frame of GFP. These fusions were constitutively expressed from the *GAL1* promoter using the GEV hybrid transcription activator. Expression was induced with the GEV inducer β-estradiol and GFP abundance was determined by immunoblotting. RNA levels were determined by quantitative RT-PCR and GFP abundance was normalized to RNA level (Figure 2B). GFP protein expression from

these plasmids differed by more than 100-fold after normalization for corresponding RNA levels. For example, the RAD27-LLT plasmid produced only about 0.03 units of GFP protein while the ZRC1-SLT construct generated over 4 units of GFP. This observation highlights the significant impact of 5' transcript leaders on translation.

As we previously found for *RTC4* (Taggart et al., 2017), the uORF-containing LLT 5' transcript leaders of *RAD27, HNT1*, and *MNT2* that are generated in zinc-deficient cells greatly decreased protein accumulation when compared to their corresponding SLT 5' transcript leader constructs (p-values of 0.02 or less). Therefore, the Zap1-mediated shift in transcription start sites for these genes may strongly inhibit protein production during zinc deficiency by affecting translation. Far lesser differences were observed for the other five pairs of transcript leaders tested. In fact, despite the presence of uORFs in the LLT 5' transcript leaders of both *FET4* and *ZAP1* that are not present in the SLT RNA, those longer leaders were translated as well as or even better than the SLT 5' transcript leaders (p-values of 0.01 and 0.06 for *FET4* and *ZAP1*, respectively). Thus, we concluded that the changes in transcription start sites mediated by Zap1 have major effects on protein accumulation in some but not all cases.

Our results suggested that the mechanisms regulating *RAD27*, *MNT2*, and *HNT1* expression were similar to that previously determined for *RTC4*. Rad27 is a DNA repair exonuclease (Reagan et al., 1995), Mnt2 is a mannosyl transferase involved in O-linked glycosylation (Romero et al., 1999), and Hnt1 is an adenosine monophosphoramidase that has been hypothesized to modulate the activity of the general transcription factor TFIIH (Bieganowski et al., 2002). Because of the potential role of Hnt1 in the global control of transcription, we focused our studies on the *HNT1* gene to further explore the mechanism of its regulation and the functional significance of that regulation to zinc-deficient cells. To characterize the effect of zinc status on *HNT1* RNA and Hnt1 protein levels, we used a GFP-tagged chromosomal allele. GFP was fused to the C-terminus of the complete *HNT1* ORF and this fusion gene is under the control of the normal *HNT1* promoter. Consistent with our previous studies implicating *HNT1* as a direct target of Zap1 regulation (Wu et al., 2008), quantitative RT-PCR showed that total *HNT1-GFP* RNA increased in zinc-deficient cells by ~2-fold relative to expression in zinc-replete cells (Figure 3A). Despite the increase in RNA abundance, however, the level of Hnt1-GFP protein decreased ~4-fold in deficient cells (Figure 3B). These results are consistent with a recent proteomics analysis that showed that native Hnt1 protein levels decrease from ~30,000 copies per cell in replete conditions to ~6000 copies in zinc-deficient cells (Wang et al., 2018).

To determine whether the decrease in Hnt1 protein abundance correlated with the transition from SLT RNA to LLT RNA production as suggested by the genome-wide transcription start site mapping, we first performed quantitative RT-PCR with primer pairs specific to either the *HNT1* ORF or the LLT 5' transcript leader sequence (Figure 4A). Consistent with the analysis of the GFP allele (Figure 3A), the *HNT1* ORF primer pair detected 1.5-2-fold increases in RNA levels during zinc deficiency for both the wild-type and GFP fusion alleles (Figure 4B). In contrast, a primer pair designed to specifically detect the LLT 5' transcript leader showed a much greater increase in zinc deficiency consistent with a shift in transcription start site. This conclusion was confirmed by Northern blotting using probes for

the *HNT1* ORF or the LLT 5' transcript leader (Figure 4A). The *HNT1* ORF probe detected a single major band in zinc-replete wild-type and *HNT1::GFP* cells that decreased in abundance in zinc-deficient cells (Figure 4C). Longer transcripts were detected in these cells when zinc deficient. That these mobility shifts represented, at least in part, the shift in expression from the SLT in zinc-replete cells to the LLT RNA in zinc-deficient cells was confirmed using an LLT 5' transcript leader-specific probe. This probe detected bands in zinc-deficient wild-type and *HNT1::GFP* fusion cells that co-migrated with the longer transcripts detected with the ORF probe. The doublet LLT bands detected in zinc deficiency may arise from the variability of *HNT1* LLT transcription start sites in zinc-deficient cells (Figure 1). An RNA was also detected with the LLT-specific probe in the *hnt1Δ* strain that was of the size expected for expression of the antibiotic resistance cassette, which replaces the *HNT1* ORF, from the *HNT1* promoter and ending at the terminator in that cassette. This conclusion was supported by the quantitative RT-PCR results (Figure 4B) in which the ORF primers detected little transcript in the *hnt1Δ* mutant while the LLT 5' transcript leader primers detected an RNA transcript in deficient mutant cells.

The paradigm of *RTC4* regulation also predicted that expression of the *HNT1* LLT RNA was dependent on Zap1 and on the candidate ZRE identified in the *HNT1* promoter. *HNT1*'s candidate ZRE (ACCTTTGAGGC) is located 268 bp upstream of the ORF initiation codon and closely matches the ZRE consensus sequence (Table 1). Using an HA epitope-tagged *HNT1* allele, we showed that LLT RNA expression was indeed highly Zap1 dependent; the LLT RNA was much reduced in a zinc-deficient *zap1Δ* mutant strain compared to the levels observed in the wild-type strain (Figure 5A). In addition, the LLT RNA was also less abundant when the ZRE in the *HNT1* promoter was mutagenized to a sequence unrelated to the consensus sequence recognized by Zap1 (Figure 5B). Surprisingly, however, zinc-responsive regulation of the *HNT1* SLT RNA was normal in *zap1Δ* mutant cells and when expressed from the ZRE mutant promoter. Moreover, immunoblotting showed that regulation of Hnt1–3xHA protein expression was also unaffected by these mutations (Figure 5C, D). These data indicate that, similar to *RTC4*, expression of the *HNT1* LLT RNA was Zap1- and ZRE-dependent. However, unlike *RTC4*, the decrease in abundance of the *HNT1* SLT RNA and the Hnt1 protein in zinc-deficient cells was not solely dependent on LLT RNA expression. We propose that other elements within the *HNT1* promoter are likely responsible for the Zap1-independent regulation of the SLT RNA by zinc.

These observations raised the question of whether the *HNT1* LLT RNA is of any functional importance given that it appeared to be dispensable for regulating *HNT1* gene expression. First, we considered the hypothesis that the *HNT1* LLT RNA was generated by a cryptic promoter that was activated by Zap1 but lacked any biological function. To assess this hypothesis, we examined the *HNT1* promoter regions of the *sensu stricto* species *Saccharomyces paradoxus* and *Saccharomyces mikatae* for conservation of the functional ZRE identified in the *S. cerevisiae* promoter (Table 1). ZRE-related sequences were found in similar upstream locations in the *HNT1* promoters of those other species and this conservation suggests that binding of Zap1 in this region has functional significance. The sequences of ZREs of verified function from the *ZRT1* and *UBI4* genes are included in Table 1 for comparison.

We also considered whether one or more of the uORFs contained in the *HNT1* LLT 5' transcript leader encodes a functional peptide. If so, expression of the LLT RNA in zinc deficiency may occur to increase the abundance of this peptide. Arguing against this hypothesis, while the upstream flanking regions of the *HNT1* genes of *S. mikatae* and *S. paradoxus* also have two or more uORFs, we could detect no conservation of amino acid sequence among the uORF-encoded peptides (data not shown). Therefore, while this hypothesis remains a formal possibility, we found no evidence to support it.

Third, because ZREs are palindromic sequences and can function bidirectionally, we assessed whether the conserved ZRE located in the region upstream of *HNT1* is present for control of the adjacent and divergently transcribed gene, *YDL124W*, rather than *HNT1*. The intergenic region between these two open reading frames is 653 base pairs and the ZRE is almost equidistant between them. If so, the *HNT1* LLT RNA might then be a nonfunctional byproduct of Zap1-mediated *YDL124W* regulation. Quantitative RT-PCR confirmed that *YDL124W* mRNA levels increased in zinc-deficient cells (Figure 6). However, this increase was even greater in a *zap1Δ* mutant strain indicating that the response was Zap1-independent. The higher induction observed in the *zap1Δ* mutant is consistent with a response to the stress of zinc deficiency, which is more severe in this mutant strain than in wild-type cells. As a positive control, we showed that the increased expression of the known Zap1-regulated gene *ZRT3* in deficient cells was dependent on Zap1. Thus, we concluded that *YDL124W*, which encodes an NADPH-dependent α-keto reductase (Chang et al., 2007), is not a Zap1-regulated gene but its expression is responsive to the stress of zinc deficiency through some other mechanism.

A fourth hypothesis arose from the recent discovery that excised linear introns of many genes are stable and accumulate in yeast cells under stress conditions to control ribosomal protein synthesis and provide stress tolerance (Morgan et al., 2019; Parenteau et al., 2019). Introns are found in ~5% of yeast genes, including *HNT1,* and the *HNT1* gene was identified as a major source of stable introns in glucose-deprived cells. These observations suggested that increased expression of the LLT RNA contributes additional excised intron levels for tolerance of zinc deficiency, perhaps in compensation for the decreased *HNT1* SLT expression in those cells. We tested this hypothesis using sensitive competitive growth assays and FACS analysis. Wild-type cells tagged with GFP were co-cultured with untagged wild-type cells or cells precisely deleted for the *HNT1* intron (*HNT1*Δi). Only the intron was removed from the genome of this strain and the *HNT1* ORF was unaffected. In addition, we tested a strain designated 5xΔi in which the introns were deleted from five genes (*ECM33, UBC4, SAC6, RFA2, HNT1*) that are major contributors to the total stable intron accumulation. Following 15 generations of growth in either zinc-replete or zinc-deficient media, the *HNT1*Δi intron deletion mutant showed no detectable difference in cell growth relative to the wild-type strain (Table 2). Moreover, the 5xΔi intron deletion strain showed a slight but detectable growth advantage in zinc deficiency. These results indicate that the *HNT1* LLT RNA and its encoded intron are not required for tolerating the stress of zinc deficiency.

A final hypothesis we evaluated was that expression of the *HNT1* LLT RNA provides a redundant mechanism to repress *HNT1* expression during zinc deficiency. When combined

with Zap1-independent regulation of the proximal *HNT1* promoter (Figure 5), LLT RNA production would ensure repression and also dampen stochastic fluctuations in expression in zinc-deficient cells (Sanchez and Golding, 2013). Alternatively, regulatory elements in the proximal *HNT1* promoter may increase expression in response to other signals or stresses, and the LLT RNA could provide a means to override that positive control and maintain low expression when zinc deficiency occurs simultaneously with other conditions. A comprehensive analysis of this hypothesis will require a more complete characterization of the proximal *HNT1* promoter and a better understanding of the Zap1-independent factors to which it responds. As a first test, we inserted the distal LLT-generating *HNT1* promoter upstream of the *GAL1* promoter driving GFP (pHNT1-pr, Figure 7A) to assess the ability of LLT RNA expression to repress a downstream promoter. It should be noted that the *GAL1* promoter fragment used in these constructs contains multiple uORFs that when present in the transcript leader would likely inhibit translation of the downstream GFP-encoding ORF. As a positive control, we inserted the distal *RTC4* LLT promoter upstream of the *GAL1* promoter (pRTC4-pr). As expected, the *RTC4* LLT promoter repressed GFP expression in zinc-deficient but not replete cells (Figure 7B, C). Similarly, the *HNT1* LLT promoter repressed GFP expression in deficient but not replete cells. These results demonstrated that transcription of the *HNT1* LLT RNA is capable of repressing a downstream promoter and are consistent with the *HNT1* LLT RNA acting to repress *HNT1* expression during zinc-deficiency. This hypothesis of LLT function also predicts that expression of *HNT1* in zinc-deficient cells may put those cells at a growth disadvantage. Consistent with that prediction, we found that *hnt1Δ* mutant cells had better growth than wild-type cells under those conditions (Table 2). Thus, even the low levels of Hnt1 expression during deficiency put the cells at a growth disadvantage related to the null mutant. A slight growth defect of the *hnt1*Δ mutant was observed in replete conditions. A *tsa1*Δ mutant was used as a positive control in this experiment and this strain showed a growth defect in replete cells that was greatly exacerbated by zinc deficiency.

DISCUSSION

It is increasingly recognized that there is a poor correlation between changes in RNA level and protein level (Ingolia et al., 2009; Lee et al., 2011) and that translatability of mRNA can vary over a wide range (Law et al., 2005; Rojas-Duran and Gilbert, 2012). RNA transcript leaders can have a tremendous impact on translation initiation and elongation and these sequences are major factors in determining translation efficiency. For example, transcript leaders can inhibit translation when they contain uORFs and/or fold into stable secondary structures. Given the impact of uORFs and secondary structure on protein expression, mechanisms that change transcription start sites, and therefore the transcript leader length and sequence, in response to stresses or other signals provide an additional layer of gene regulation over and above simply changing RNA abundance. We can envision two general types of effects resulting from induced changes in transcription start sites, i.e. changes that increase translatability of 5’ transcript leaders that enhance the effects of any transcriptional activation increasing RNA abundance, and changes that reduce translatability and thereby inhibit protein expression. The changes in transcription start sites of *RTC4*, *RAD27*, *MNT2*, and *HNT1* are consistent with that latter model. An example of the first scenario of

enhancing expression in response to zinc deficiency was observed for *ZRC1*. This positive effect makes biological sense because of the importance of increasing Zrc1 protein levels in zinc deficiency to tolerate “zinc shock”, the high level of zinc uptake when the metal is resupplied to a deficient cell (MacDiarmid et al., 2003).

There are many examples of regulated changes in transcription start site that are emerging, and these highlight that such changes are a common but largely unrecognized aspect of gene regulation. For example, treating yeast with mating pheromone caused changes in translation efficiency of approximately 200 genes and many of those effects were linked to alterations in transcription start sites (Law et al., 2005). Also, in a study examining transcription start sites in yeast exposed to 18 different stress conditions, over 800 genes showed altered sites of transcription initiation in response to one or more stress condition (Waern and Snyder, 2013). Among these, 446 genes showed changes in transcription start sites that affected the inclusion of uORFs in their 5’ transcript leaders. More specific examples in which the transcription factors mediating the change are known include the regulation of the *tco1+* gene in *Schizosaccharomyces pombe* (Sehgal et al., 2008) and the *NDC80* gene of *S. cerevisiae* in which induced expression of uORF-containing RNAs shut off expression of shorter, well-translated RNA (Chia et al., 2017). This type of regulation is not limited to yeasts; the human oncogene *MDM2* is regulated in a similar fashion (Hollerer et al., 2019). Thus, we contend that alternate transcription start sites with altered translation efficiencies likely affect gene/protein expression in many organisms.

In our study we detected some genes for which activation by Zap1 shifted transcription from start sites proximal to the protein-encoding ORF to more distal sites (*HNT1, MNT2, RAD27*, and *RTC4*) and other cases where Zap1 action shifted the start site closer to the ORF (*FET4, MCD4, ZAP1, ZRC1, ZRT3*). We suspect that one major factor in determining the direction of these shifts is the position of the ZRE within the promoter. For all genes where the Zap1-mediated shift was to a more distal site, the ZRE is located far (>250 bp) from the ORF. For those that shifted closer to the ORF, the ZRE is also closer (<200 bp) to the ORF. The lone exception to this correlation is *FET4*, in which the ZRE is ~400 bp upstream but the shift is to quite close to the ORF. The reasons for this unusual behavior are not clear but it may reflect the specific positioning of other regulatory and/or basal transcription (e.g. TATA) elements in this promoter.

The effects of uORFs in the transcript leaders also showed a pattern of which inhibited translation and which did not. Of the six genes with uORF-containing RNAs, uORFs correlated with lower translation efficiency in four cases (*RTC4, RAD27, MNT2, HNT1*) but not in two cases (*FET4, ZAP1*). The LLT transcripts of *FET4* and *ZAP1* contain only one uORF while the LLT transcripts of the other genes contain two or more. This suggests that the number of uORFs influences their translatability. The position of the uORFs within the 5’ transcript leaders, codon usage within the uORF, the surrounding secondary structures, and sequences flanking the uORF AUG codons may also influence their inhibitory effect on translation of downstream ORFs (Lin et al., 2019; Wethmar, 2014).

Our results suggested that the observed shifts in transcription start site caused decreased expression of Rad27, Mnt2, and Hnt1 due to the reduced translation efficiency of the longer

transcript leaders. Consistent with this hypothesis, Rad27 protein levels drop in zinc deficiency despite the increase in RNA (Taggart et al., 2017). Similarly, Hnt1 protein levels also drop in deficient cells but, in contrast to *RTC4*, we were surprised to find that the decrease in SLT production is Zap1- and ZRE-independent. This observation raised the question about the function of the LLT transcript. We present evidence that LLT production likely has some functional significance; the ZRE and presence of uORFs are conserved among other *Saccharomyces* species. After testing and eliminating several other hypotheses, we propose that the LLT RNA provides a second mechanism to shut off the SLT RNA. This could either serve as a fail-safe mechanism to ensure repression of Hnt1 production or, alternatively, provide an override switch to shut off Hnt1 production in zinc-deficient cells when other stressors or signals are promoting its synthesis. The Zap1-independent mechanism that reduces Hnt1 in zinc deficiency remains unclear.

A remaining unanswered question is what is the function of the Hnt1 protein and what purpose does its downregulation serve in zinc-deficient cells? Given the conservation of *HNT1* and its mammalian orthologs, this is an important question for understanding both how cells respond to zinc deficiency and also how the loss of Hint1 function leads to an inherited form of peripheral neuropathy. Hnt1 and Hint1 are members of the histidine triad superfamily of nucleotide hydrolases and nucleotide transferases (Huebner et al., 2011). Histidine triad proteins contain a characteristic His-x-His-x-His-x-x motif where x is a hydrophobic residue. This motif is contained within a nucleotide-binding cleft and these proteins hydrolyze many different nucleotide substrates in vitro. The in vivo substrate(s) of this enzymatic activity are not yet known. One proposed function of Hnt1 is as a modulator of Kin28/Cdk7 activity (Bieganowski et al., 2002). Kin28/Cdk7 is a component of general transcription factor TFIIH which phosphorylates the C-terminal domain of RNA polymerase II to free the polymerase from the preinitiation complex at the gene's promoter. It was proposed that the hydrolytic activity of Hnt1 and Hint1 eliminates the accumulation of a nucleotide metabolite that inhibits TFIIH function. If this model is correct, decreased Hnt1 abundance in zinc deficiency may decrease expression of the ~500 Kin28-sensitive genes in the genome by allowing the inhibitory metabolite to accumulate (Wong et al., 2014). Thus, repression of Hnt1 in zinc-deficient cells may be one component of a mechanism that globally regulates transcription. Alternatively, mammalian Hint1 acts to suppress transcription by directly or indirectly inhibiting specific transcription factors, e.g. MITF, USF2, AP-1 (Lee and Razin, 2005; Motzik et al., 2017; Wang et al., 2007). According to this model, down-regulation of Hnt1 would be expected to affect genes regulated by a specific yeast transcription factor. A third model is provided by the observation that Hint1 aids crosstalk between G-protein coupled receptors (Rodriguez-Munoz et al., 2016). Hnt1 has a conserved zinc-binding domain so its reduced expression may be a zinc-sparing response to reduce the zinc requirement of zinc deficient cells (Jung et al., 2019). The abundance of Hnt1 decreases markedly during deficiency (Wang et al., 2018). Moreover, members of the broader histidine triad superfamily have been implicated in zinc homeostasis suggesting a possible role for Hnt1 in these processes (Moulin et al., 2019). Future experiments will test these models to probe how *HNT1* regulation impacts gene expression and cell physiology during zinc deficiency.

EXPERIMENTAL PROCEDURES

Strains and growth conditions-

Yeast strains used in this work were BY4743 (*MATa/MATα his3Δ1/his3Δ1 leu2Δ0/leu2Δ0 lysΔ0/LYS2 MET15/met15Δ0 ura3Δ0/ura3Δ0*) and its isogenic mutant strains BY4743 *zap1Δ*::*KanMX* and BY4743 *hnt1Δ*::*KanMX*, DY1457 (*MATa ade6 can1 his3 leu2 trp1 ura3*), BY4741 (*MATa his3 leu2 met15 ura3*), BY4741 *HNT1*::GFP (Thermo Fisher Scientific), BY4741 *HNT1Δintron* (*HNT1*Δi, D. Bartel, MIT) and BY4741 *ECM33Δintron UBC4Δintron HNT1Δintron SAC6Δintron RFA2Δintron* (5xΔi, D. Bartel, MIT). Media used were YPD (1% yeast extract/ 2% peptone/ 2% glucose), synthetic defined (SD, 0.67% yeast nitrogen base), and low zinc medium (LZM) prepared as described previously (Zhao and Eide, 1996). LZM contains 20 mM citrate and 1 mM EDTA to buffer pH and zinc availability, respectively. While EDTA is not a zinc-specific chelator, the effect of zinc supplements up to 100 μM on the availability of other metal nutrients is minimal. The zinc-deficient condition used was LZM + 1 μM $ZnCl_2$ and the zinc-replete condition used was LZM +100 μM $ZnCl_2$.

Plasmid constructions-

The *GAL1*-driven SLT-GFP and LLT-GFP plasmids were constructed by PCR amplification of fragments corresponding to the SLT and LLT 5' transcript leaders of the following genes (the number in parentheses is the distal endpoint of the fragment with $^{+}1$ representing the A of the initiation codon): *RAD27*: $^{-}$23 (SLT), $^{-}$181 (LLT) bp, *HNT1*: $^{-}$34 (SLT), $^{-}$113 (LLT) bp, *MNT2*: $^{-}$109 (SLT), $^{-}$214 (LLT) bp, *FET4*: $^{-}$1 (SLT), $^{-}$133 (LLT) bp, *ZAP1*: $^{-}$8 (SLT), $^{-}$72 (LLT) bp, *MCD4*: $^{-}$5 (SLT), $^{-}$42 (LLT) bp, *ZRC1*: $^{-}$17 (SLT), $^{-}$125 (LLT) bp and *ZRT3*: $^{-}$19 (SLT), $^{-}$46 (LLT). Those fragments were inserted with GFP into pRS316-GAL1 (Liu et al., 1992) by homologous recombination. It should be noted that the *HNT1* SLT mRNA starts at a site between the first and second ATG codons of the protein-coding open reading frame indicating that the second ATG is the actual initiation codon (Figure 2). To generate pHNT1–3xHA, a plasmid expressing three copies of the hemagglutinin antigen (HA) fused to the *HNT1* C-terminus, the *HNT1* gene was amplified from chromosomal DNA with 921 bp of upstream DNA flanking the *HNT1* ORF and inserted between the *Bam*HI and *Eco*RI sites of pFL38-ZRC1–3XHA (MacDiarmid et al., 2002) by homologous recombination. pHNT1–3xHA^{mZRE} was constructed by amplifying fragments from BY4743 with transversion mutations introduced into the *HNT1 ZRE* by overlap PCR. The sequence of the wild-type *HNT1* ZRE is ACCTTTGAGGC and the mZRE mutant sequence is CAAGGGTCTTA. Plasmid pPGK1-ZRT1 was previously described (Bird et al., 2006b).

pRTC4-pr and pHNT1-pr were constructed by PCR amplifying their distal LLT promoters spanning from −766 (*HNT1*) or −805 (*RTC4*) to 10 bp beyond the start site of their LLT RNAs and inserting them by homologous recombination into the *Eco*RI site of pMCD4-LLT-GFP (labeled pGAL-GFP in Figure 7) described above. In this vector, GFP plus 42 bp of *MCD4* 5' transcript leader is expressed from the *GAL1* promoter.

Quantitative RT-PCR analysis-

RNA extraction and quantitative RT-PCR analysis was performed using a previously described protocol (MacDiarmid et al., 2016). Primer pairs used were (5'−3'): TGCCATGTGGTAATCCCAGC and TGTCCACACAATCTGCCCT for GFP, TGTGTGTTCGACTGGAAAGC and CATCAATGTTTCTTAAAAGTCTG for the *HNT1* LLT 5' transcript leader, CTACGCTTGATGCTGCCTGT and TGACCTTCAGCAGTAGGTTGGA for the *HNT1* open reading frame, and TTGGCTCTGATGTCTCGTCAA, GCCATCATTGGGACAGGTACTAG and GTGCCTTCCCAACTTCTGGAT for *YDL124W*, and TGAGCGTTACTGCAGGGTTC and GTGCCTGAGCTATGGGACTG for *ZRT3*. The average C_t values for three control genes (*TAF10, ACT1* and *CMD1*) was used to normalize the expression of target genes. These control genes were selected from multiple candidate genes tested for their highly stable expression under the conditions used in our experiments (data not shown).

Northern blot analysis-

Northern blot analysis was done as previously described (MacDiarmid et al., 2016). To make strand-specific antisense probes, PCR fragments of the *HNT1, GFP,* and *TAF10* genes were amplified from genomic DNA, introducing the T7 RNA polymerase promoter into the products in the antisense orientation by including it in the downstream primer. Probe primer sequences were (5'-3'): GAAGCATTGCTGTACGATCG and agttaatacgactcactatagggaTCCATCAATGTTTCTTAAAAGTCTGGA for the *HNT1* LLT 5' transcript leader, CCTAAGTACCATGGTGCGAA and agttaatacgactcactatagggaGTAGCTTGCCCAACTTATCGAA for the *HNT1* ORF, GGATCCGCTGGCTCCGCT and agttaatacgactcactatagggaTTAAGCGTAATCTGGAACGTCATATGGA for the 3xHA tag, and ATGGATTTTGAGGAAGATTAC and agttaatacgactcactatagggaCTAACGATAAAAGTCTGGGCG for *TAF10*. Lowercase letters indicated the common T7 promoter portion of each primer set.

Immunoblot analysis-

Protein extracts were prepared using an extraction protocol as previously described (MacDiarmid et al., 2013). SDS-PAGE and immunoblotting were conducted using a Li-Cor Odyssey infrared dye detection system as previously described (MacDiarmid et al., 2013). Antibodies used were anti-GFP (Roche, product number 11814460001), anti-HA (12CA5, Roche, product number 11583816001), anti-Vma1 (Invitrogen, product number A-6427) and anti-Pgk1 (Abcam, product number 22C5D8). IR680 dye-labeled secondary anti-mouse antibody (product number 680LT) was obtained from LiCor.

Data processing and statistical analysis-

Immunoblot and Northern blot band intensities were quantified using Image Studio software (Li-Cor). For experiments in which protein accumulation was normalized to mRNA levels, values of standard deviation were calculated, and statistical significance was assessed using Student's t-test.

ACKNOWLEDGEMENTS

This work was supported by National Institutes of Health grant RO1-GM56285 (D.E.) and a Science Achievement Scholarship of Thailand (S.T.). The authors thank David Bartel (MIT) for providing the intron deletion strains. FACS analysis was performed at the University of Wisconsin Carbone Cancer Center Flow Cytometry Laboratory.

REFERENCES

Arribere JA, and Gilbert WV. 2013 Roles for transcript leaders in translation and mRNA decay revealed by transcript leader sequencing. Genome Res. 23:977–987. [PubMed: 23580730]

Bieganowski P, Garrison PN, Hodawadekar SC, Faye G, Barnes LD, and Brenner C. 2002 Adenosine monophosphoramidase activity of Hint and Hnt1 supports function of Kin28, Ccl1, and Tfb3. J. Biol. Chem 277:10852–10860. [PubMed: 11805111]

Bird AJ, Gordon M, Eide DJ, and Winge DR. 2006a Repression of ADH1 and ADH3 during zinc deficiency by Zap1-induced intergenic RNA transcripts. EMBO J. 25:5726–5734. [PubMed: 17139254]

Bird AJ, Swierczek S, Qiao W, Eide DJ, and Winge DR. 2006b Zinc metalloregulation of the zinc finger pair domain. J. Biol. Chem 281:25326–25335. [PubMed: 16829533]

Chang Q, Griest TA, Harter TM, and Petrash JM. 2007 Functional studies of aldo-keto reductases in Saccharomyces cerevisiae. Biochim. Biophys. Acta 1773:321–329. [PubMed: 17140678]

Chia M, Tresenrider A, Chen J, Spedale G, Jorgensen V, Unal E, and van Werven FJ. 2017 Transcription of a 5' extended mRNA isoform directs dynamic chromatin changes and interference of a downstream promoter. eLife. doi: 10.7554/eLife.27420

De Nicola R, Hazelwood LA, De Hulster EA, Walsh MC, Knijnenburg TA, Reinders MJ, Walker GM, Pronk JT, Daran JM, and Daran-Lapujade P. 2007 Physiological and transcriptional responses of Saccharomyces cerevisiae to zinc limitation in chemostat cultures. Appl. Environ. Microbiol 73:7680–7692. [PubMed: 17933919]

Eide DJ 2009 Homeostatic and adaptive responses to zinc deficiency in Saccharomyces cerevisiae. J. Biol. Chem 284:18565–18569. [PubMed: 19363031]

Frey AG, Bird AJ, Evans-Galea MV, Blankman E, Winge DR, and Eide DJ. 2011 Zinc-regulated DNA binding of the yeast Zap1 zinc-responsive activator. PloS One. 6:e22535. [PubMed: 21799889]

Hollerer I, Barker JC, Jorgensen V, Tresenrider A, Dugast-Darzacq C, Chan LY, Darzacq X, Tjian R, Unal E, and Brar GA. 2019 Evidence for an integrated gene repression mechanism based on mRNA isoform toggling in human cells. G3. 9:1045–1053. [PubMed: 30723103]

Huebner K, Saldivar JC, Sun J, Shibata H, and Druck T. 2011 Hits, Fhits and Nits: beyond enzymatic function. Adv. Enzyme Regul 51:208–217. [PubMed: 21035495]

Ingolia NT, Ghaemmaghami S, Newman JR, and Weissman JS. 2009 Genome-wide analysis in vivo of translation with nucleotide resolution using ribosome profiling. Science. 324:218–223. [PubMed: 19213877]

Jung A, Yun JS, Kim S, Kim SR, Shin M, Cho DH, Choi KS, and Chang JH. 2019 Crystal structure of histidine triad nucleotide-binding protein from the pathogenic fungus Candida albicans. Mol. Cells 42:56–66. [PubMed: 30622225]

Korsisaari N, and Makela TP. 2000 Interactions of Cdk7 and Kin28 with Hint/PKCI-1 and Hnt1 histidine triad proteins. J. Biol. Chem 275:34837–34840. [PubMed: 10958787]

Law GL, Bickel KS, MacKay VL, and Morris DR. 2005 The undertranslated transcriptome reveals widespread translational silencing by alternative 5' transcript leaders. Genome Biol. 6:R111. [PubMed: 16420678]

Lee MV, Topper SE, Hubler SL, Hose J, Wenger CD, Coon JJ, and Gasch AP. 2011 A dynamic model of proteome changes reveals new roles for transcript alteration in yeast. Mol. Syst. Biol 7:514. [PubMed: 21772262]

Lee YN, and Razin E. 2005 Nonconventional involvement of LysRS in the molecular mechanism of USF2 transcriptional activity in FcepsilonRI-activated mast cells. Mol. Cell. Biol 25:8904–8912. [PubMed: 16199869]

Lin Y, May GE, Kready H, Nazzaro L, Mao M, Spealman P, Creeger Y, and McManus CJ. 2019 Impacts of uORF codon identity and position on translation regulation. Nucl. Acids Res doi: 10.1093/nar/gkz681

Liu H, Krizek J, and Bretscher A. 1992 Construction of a GAL1-regulated yeast cDNA expression library and its application to the identification of genes whose overexpression causes lethality in yeast. Genetics. 132:665–673. [PubMed: 1468625]

Lyons TJ, Gasch AP, Gaither LA, Botstein D, Brown PO, and Eide DJ. 2000 Genome-wide characterization of the Zap1p zinc-responsive regulon in yeast. Proc. Natl. Acad. Sci. USA 97:7957–7962. [PubMed: 10884426]

MacDiarmid CW, Milanick MA, and Eide DJ. 2002 Biochemical properties of vacuolar zinc transport systems of Saccharomyces cerevisiae. J. Biol. Chem 277:39187–39194. [PubMed: 12161436]

MacDiarmid CW, Milanick MA, and Eide DJ. 2003 Induction of the ZRC1 metal tolerance gene in zinc-limited yeast confers resistance to zinc shock. J. Biol. Chem 278:15065–15072. [PubMed: 12556516]

MacDiarmid CW, Taggart J, Jeong J, Kerdsomboon K, and Eide DJ. 2016 Activation of the yeast UBI4 polyubiquitin gene by Zap1 transcription factor via an intragenic promoter is critical for zinc-deficient growth. J. Biol. Chem 291:18880–18896. [PubMed: 27432887]

MacDiarmid CW, Taggart J, Kerdsomboon K, Kubisiak M, Panascharoen S, Schelble K, and Eide DJ. 2013 Peroxiredoxin chaperone activity is critical for protein homeostasis in zinc-deficient yeast. J. Biol. Chem 288:31313–31327. [PubMed: 24022485]

Morgan JT, Fink GR, and Bartel DP. 2019 Excised linear introns regulate growth in yeast. Nature. 565:606–611. [PubMed: 30651636]

Motzik A, Amir E, Erlich T, Wang J, Kim BG, Han JM, Kim JH, Nechushtan H, Guo M, Razin E, and Tshori S. 2017 Post-translational modification of HINT1 mediates activation of MITF transcriptional activity in human melanoma cells. Oncogene. 36:4732–4738. [PubMed: 28394346]

Moulin P, Rong V, Ribeiro ESA, Pederick VG, Camiade E, Mereghetti L, McDevitt CA, and Hiron A. 2019 Defining the role of the Streptococcus agalactiae Sht-family proteins in zinc acquisition and complement evasion. J. Bacteriol doi: 10.1128/JB.00757-18

Parenteau J, Maignon L, Berthoumieux M, Catala M, Gagnon V, and Abou Elela S. 2019 Introns are mediators of cell response to starvation. Nature. 565:612–617. [PubMed: 30651641]

Pickering BM, and Willis AE. 2005 The implications of structured 5' untranslated regions on translation and disease. Sem. Cell Dev. Biol 16:39–47.

Reagan MS, Pittenger C, Siede W, and Friedberg EC. 1995 Characterization of a mutant strain of Saccharomyces cerevisiae with a deletion of the RAD27 gene, a structural homolog of the RAD2 nucleotide excision repair gene. J. Bacteriol 177:364–371. [PubMed: 7814325]

Rodriguez-Munoz M, Sanchez-Blazquez P, Merlos M, and Garzon-Nino J. 2016 Endocannabinoid control of glutamate NMDA receptors: the therapeutic potential and consequences of dysfunction. Oncotarget. 7:55840–55862. [PubMed: 27323834]

Rojas-Duran MF, and Gilbert WV. 2012 Alternative transcription start site selection leads to large differences in translation activity in yeast. RNA. 18:2299–2305. [PubMed: 23105001]

Romero PA, Lussier M, Veronneau S, Sdicu AM, Herscovics A, and Bussey H. 1999 Mnt2p and Mnt3p of Saccharomyces cerevisiae are members of the Mnn1p family of alpha-1,3-mannosyltransferases responsible for adding the terminal mannose residues of O-linked oligosaccharides. Glycobiology. 9:1045–1051. [PubMed: 10521541]

Sanchez A, and Golding I. 2013 Genetic determinants and cellular constraints in noisy gene expression. Science. 342:1188–1193. [PubMed: 24311680]

Sehgal A, Hughes BT, and Espenshade PJ. 2008 Oxygen-dependent, alternative promoter controls translation of tco1+ in fission yeast. Nucl. Acids Res 36:2024–2031. [PubMed: 18276645]

Singh N, Yadav KK, and Rajasekharan R. 2017 Effect of zinc deprivation on the lipid metabolism of budding yeast. Curr. Genet 63:977–982. [PubMed: 28500379]

Taggart J, MacDiarmid CW, Haws S, and Eide DJ. 2017 Zap1-dependent transcription from an alternative upstream promoter controls translation of RTC4 mRNA in zinc-deficient Saccharomyces cerevisiae. Mol. Microbiol 106:678–689. [PubMed: 28963784]

Taggart J, Wang Y, Weisenhorn E, MacDiarmid CW, Russell J, Coon JJ, and Eide DJ. 2018 The GIS2 Gene Is Repressed by a Zinc-Regulated Bicistronic RNA in Saccharomyces cerevisiae. Genes (Basel). doi: 10.3390/genes9090462

Vogel C, and Marcotte EM. 2012 Insights into the regulation of protein abundance from proteomic and transcriptomic analyses. Nat. Rev. Genet 13:227–232. [PubMed: 22411467]

Waern K, and Snyder M. 2013 Extensive transcript diversity and novel upstream open reading frame regulation in yeast. G3. 3:343–352. [PubMed: 23390610]

Wang L, Zhang Y, Li H, Xu Z, Santella RM, and Weinstein IB. 2007 Hint1 inhibits growth and activator protein-1 activity in human colon cancer cells. Cancer Res. 67:4700–4708. [PubMed: 17510397]

Wang Y, Weisenhorn E, MacDiarmid CW, Andreini C, Bucci M, Taggart J, Banci L, Russell J, Coon JJ, and Eide DJ. 2018 The cellular economy of the Saccharomyces cerevisiae zinc proteome. Metallomics. 10:1755–1776. [PubMed: 30358795]

Wethmar K 2014 The regulatory potential of upstream open reading frames in eukaryotic gene expression. RNA. 5:765–778. [PubMed: 24995549]

Wong KH, Jin Y, and Struhl K. 2014 TFIIH phosphorylation of the Pol II CTD stimulates mediator dissociation from the preinitiation complex and promoter escape. Mol. Cell 54:601–612. [PubMed: 24746699]

Wu CY, Bird AJ, Chung LM, Newton MA, Winge DR, and Eide DJ. 2008 Differential control of Zap1-regulated genes in response to zinc deficiency in Saccharomyces cerevisiae. BMC Genomics. 9:370. [PubMed: 18673560]

Wu CY, Roje S, Sandoval FJ, Bird AJ, Winge DR, and Eide DJ. 2009 Repression of sulfate assimilation is an adaptive response of yeast to the oxidative stress of zinc deficiency. J. Biol. Chem 284:27544–27556. [PubMed: 19656949]

Wu YH, Taggart J, Song PX, MacDiarmid C, and Eide DJ. 2016 An MSC2 promoter-lacZ fusion gene reveals zinc-responsive changes in sites of transcription initiation that occur across the yeast genome. PloS One. 11:e0163256. [PubMed: 27657924]

Zhao H, and Eide D. 1996 The yeast ZRT1 gene encodes the zinc transporter protein of a high-affinity uptake system induced by zinc limitation. Proc. Natl. Acad. Sci. USA 93:2454–2458. [PubMed: 8637895]

Zimon M, Baets J, Almeida-Souza L, De Vriendt E, Nikodinovic J, Parman Y, Battaloglu E, Matur Z, Guergueltcheva V, Tournev I, Auer-Grumbach M, De Rijk P, Petersen BS, Muller T, Fransen E, Van Damme P, Loscher WN, Barisic N, Mitrovic Z, Previtali SC, Topaloglu H, Bernert G, Beleza-Meireles A, Todorovic S, Savic-Pavicevic D, Ishpekova B, Lechner S, Peeters K, Ooms T, Hahn AF, Zuchner S, Timmerman V, Van Dijck P, Rasic VM, Janecke AR, De Jonghe P, and Jordanova A. 2012 Loss-of-function mutations in HINT1 cause axonal neuropathy with neuromyotonia. Nat. Genet 44:1080–1083. [PubMed: 22961002]

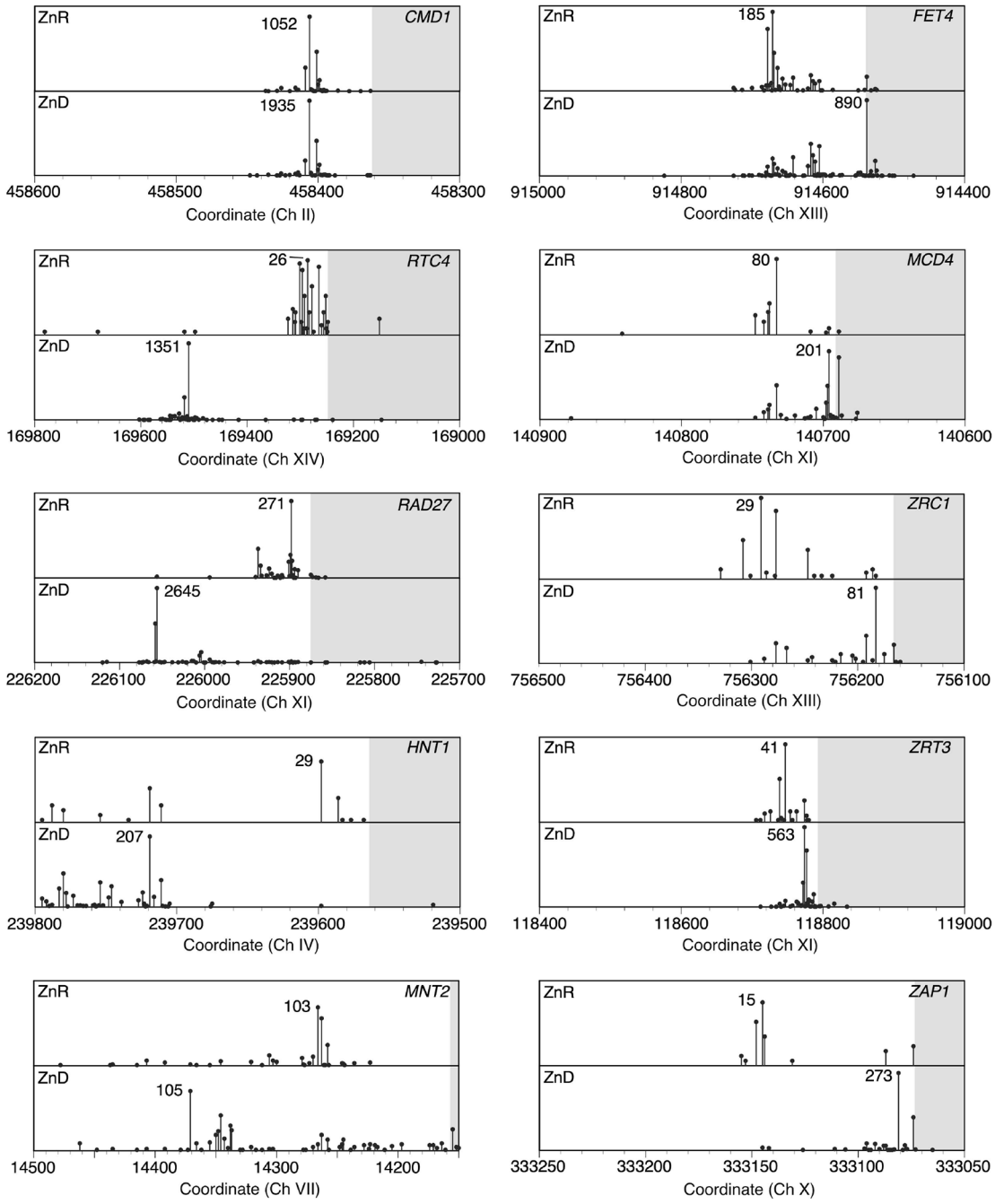

Figure 1. Zinc status alters the transcription start sites of several Zap1-regulated genes.

Transcription start sites mapped by Deep-RACE for the indicated genes under zinc-replete (LZM + 100 μM $ZnCl_2$, ZnR) and zinc-deficient (LZM + 1 μM $ZnCl_2$ ZnD) conditions are plotted relative to the amino-terminal ends of their open reading frames shown in gray. The number of independent sequencing reads representing RNA 5' ends are plotted across each region. The x-axis coordinates represent the location on the corresponding chromosomes. For scale, peak values of the number of independent sequence reads for each gene and

growth condition are shown. The data shown are from a prior genome-wide study (Wu et al., 2016).

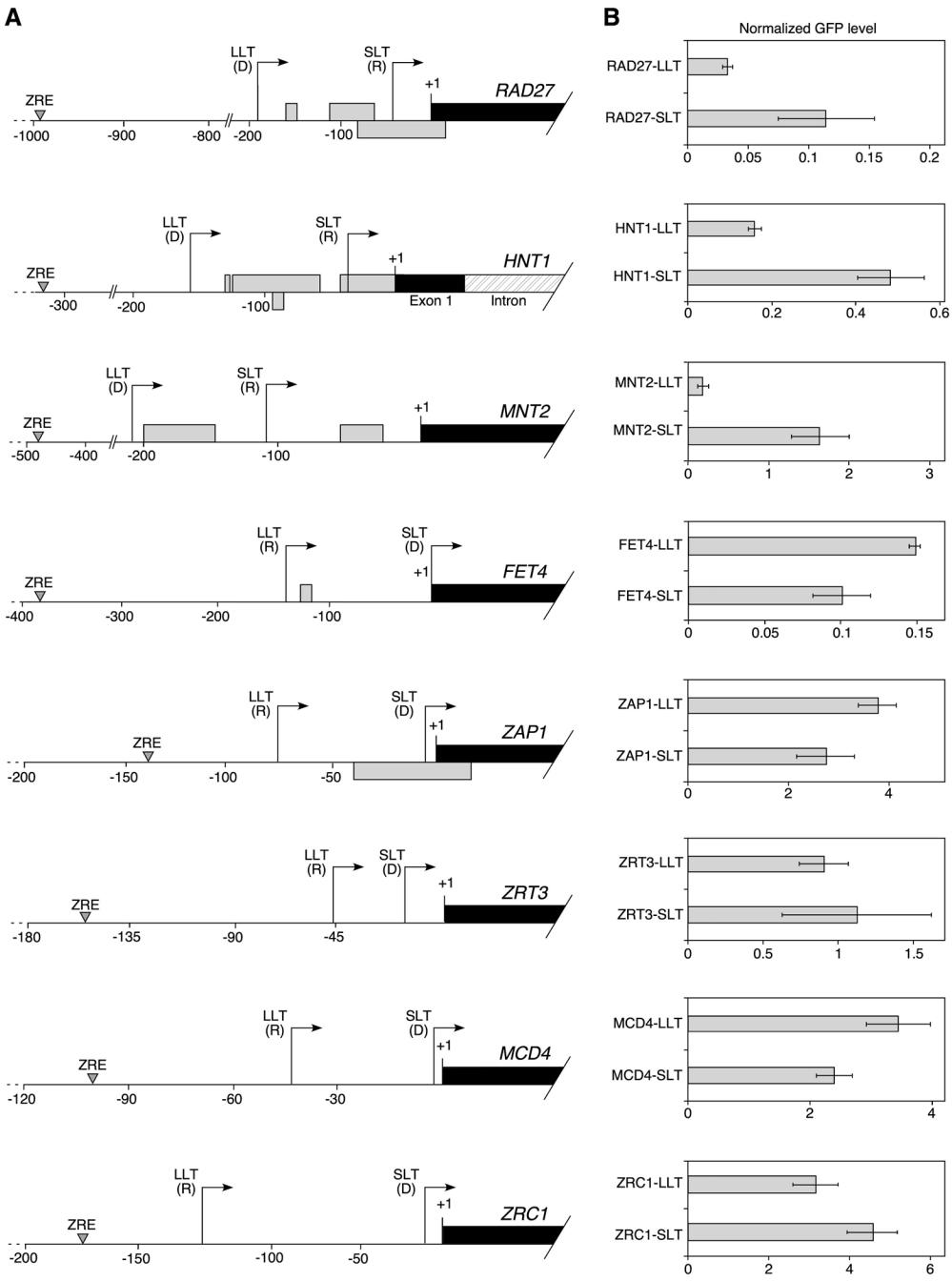

Figure 2. Effect of different 5' transcript leaders on translation.

A) The major SLT and LLT transcription start sites mapped for the indicated genes in zinc-replete (R) and deficient (D) cells are plotted relative to the translation initiation codon of each gene's ORF (numbered as +1). The positions of the ZREs (*triangles*), upstream open reading frames in the transcript leaders (*gray* boxes), protein-coding open reading frames (*black* boxes), and the location of *HNT1* exon 1 and intron are also shown. B) The abundance of GFP protein normalized to RNA abundance was plotted to evaluate the translation efficiency of each transcript leader. Wild-type (DY1475) cells were transformed

with plasmids encoding either the indicated long leader transcripts (LLT) or short leader transcripts (SLT) fused to GFP and expressed from the *GAL1* promoter. Cells were grown in the zinc-replete LZM + 100 μM $ZnCl_2$ medium prior to quantitative RT-PCR and immunoblotting. The data shown are the means ± 1 S.D. for three biological replicates. The p-values were 0.02, 0.002, 0.004, 0.01, 0.06, 0.5, 0.04, and 0.04 for *RAD27, HNT1, MNT2, FET4, ZAP1, ZRT3, MCD4*, and *ZRC1* LLT vs. SLT, respectively. Therefore, all differences between SLT and LLT constructs were statistically significant (p-value <0.05) with the exception of the *ZAP1*- and *ZRT3*-derived constructs.

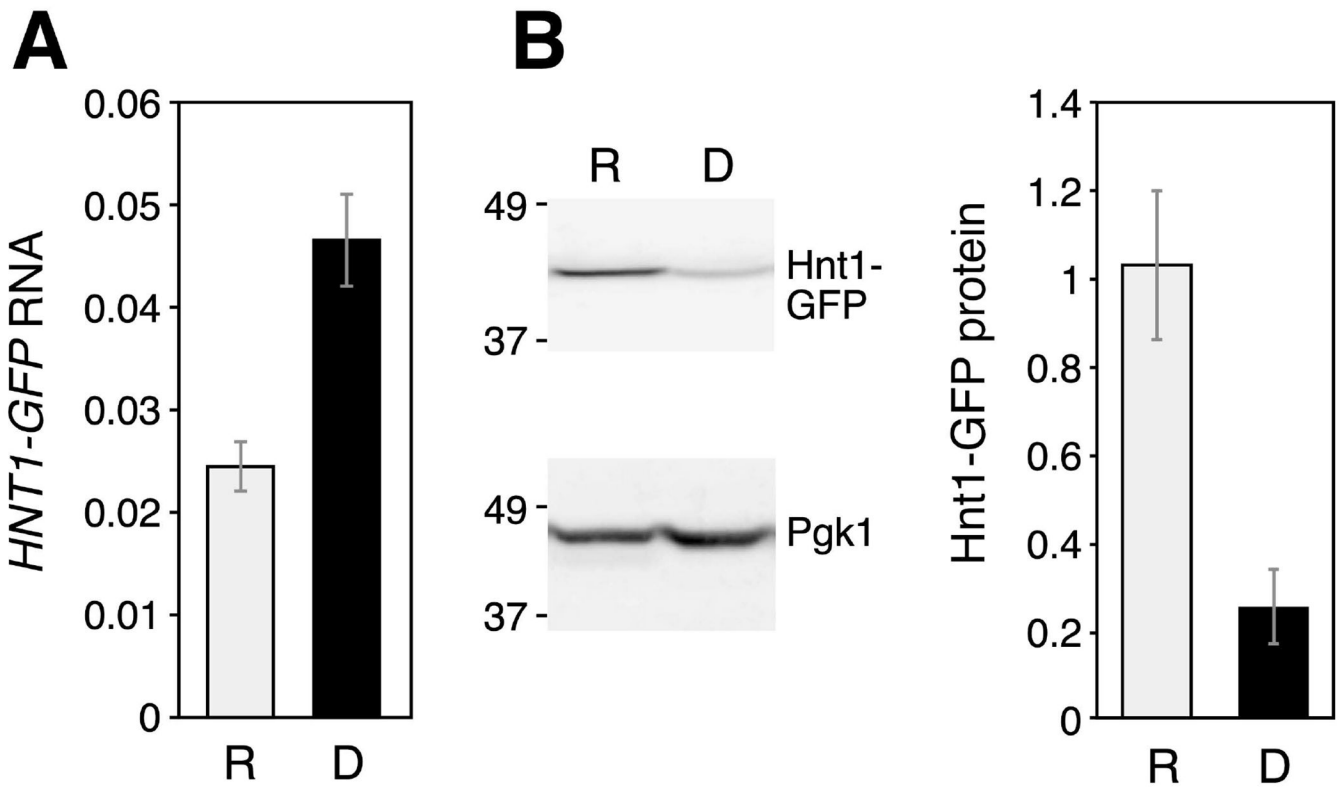

Figure 3. Opposite regulation of *HNT1* RNA and Hnt1 protein accumulation in response to zinc status.

A wild-type strain (BY4741) with an *HNT1* C-terminal GFP fusion allele was grown in LZM + 100 μM $ZnCl_2$ (zinc-replete, R) and LZM + 1 μM $ZnCl_2$ (zinc-deficient, D) media prior to analysis by (A) quantitative RT-PCR and (B) immunoblotting with anti-GFP and anti-Pgk1 antibodies. One representative immunoblot is shown in panel B and Pgk1 was included as a loading control. The locations of molecular mass markers (kDa) are indicated on the left side of each blot. For both panels, the data averaged from three biological replicates are shown and the error bars denote ± 1 S.D.

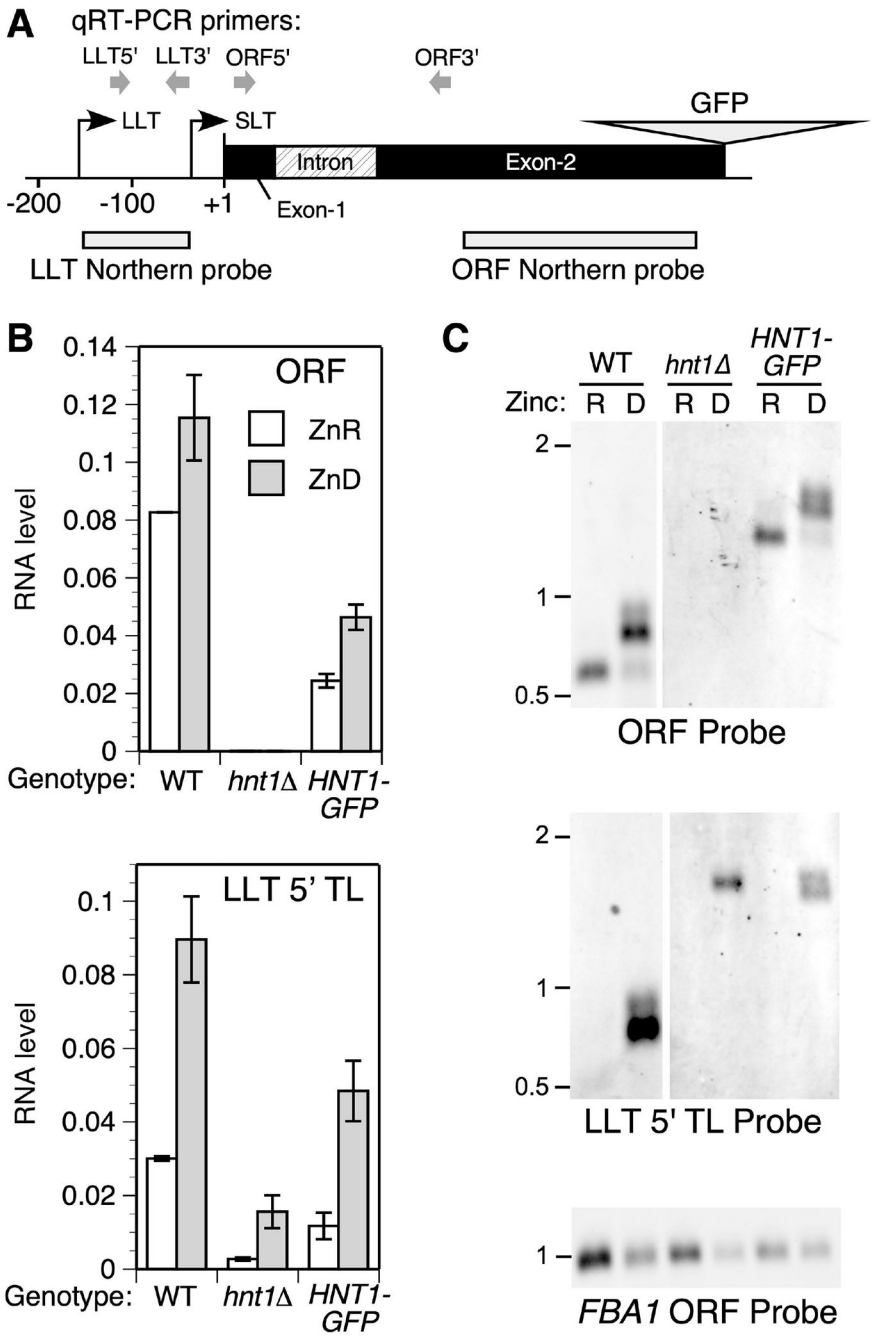

Figure 4. The effect of zinc status on the transcription start sites of *HNT1*.

Wild-type (BY4743), *hnt1Δ* (BY4743 *hnt1Δ::KanMX*) and *HNT1::GFP* (BY4741 *HNT1::GFP*) cells were grown in LZM + 100 μM $ZnCl_2$ (zinc-replete, R) and LZM + 1 μM $ZnCl_2$ (zinc-deficient, D) media prior to analysis. A) Diagram showing the location of RT-PCR primers and Northern blot probes used in this experiment. B) Quantitative RT-PCR analysis using a primer pair that detects the *HNT1* ORF (*top* panel) or the LLT 5' transcript leader (*bottom* panel). The abundance of these RNA are plotted as the average of three biological replicates and the error bars denote ± 1 S.D. C) Northern blot analysis using a

probe for the *HNT1* ORF or a probe specific to the LLT transcript leader. The blots shown are representatives of three biological replicate blots each with similar results. A probe for *FBA1* RNA was used to confirm sample loading in all lanes and the locations of size markers (kb) are indicated on the left side of the blots. The *HNT1* ORF and LLT 5' transcript leader (TL) blots are split because the portions containing lanes 1 and 2 were scanned at a lower intensity than the portions containing lanes 3-6 due to the differences in RNA abundance among the alleles.

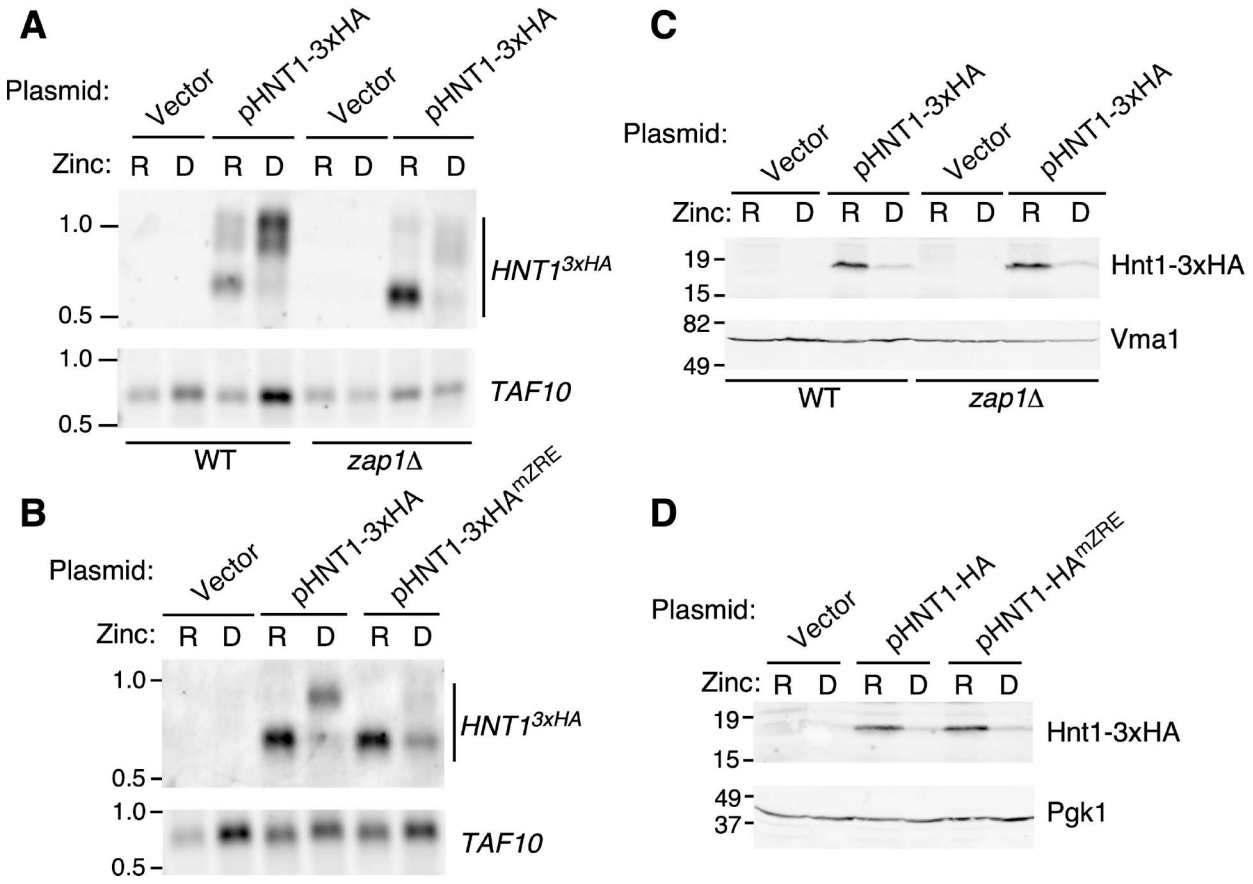

Figure 5. Expression of the *HNT1* LLT RNA is Zap1- and ZRE-dependent while zinc-responsive regulation of the *HNT1* SLT RNA and Hnt1 protein are not.

Wild-type (BY4743) and *zap1Δ* (BY4743 *zap1Δ::KanMX*) mutant cells were transformed with the empty plasmid vector, pHNT1–3xHA, or pHNT1–3xHA^{mZRE}. Cells were grown in LZM + 100 μM $ZnCl_2$ (zinc-replete, R) and LZM + 1 μM $ZnCl_2$ (zinc-deficient, D) media prior to Northern blot analysis with an HA tag-specific probe (A, B) and immunoblotting using anti-HA antibody (C, D). *TAF10* and Pgk1/Vma1 were used as loading controls for the Northern blots and immunoblots, respectively. The locations of size markers (kb, kDa) are indicated on the left side of the blots. Shown are representatives of three biological replicate blots each with similar results.

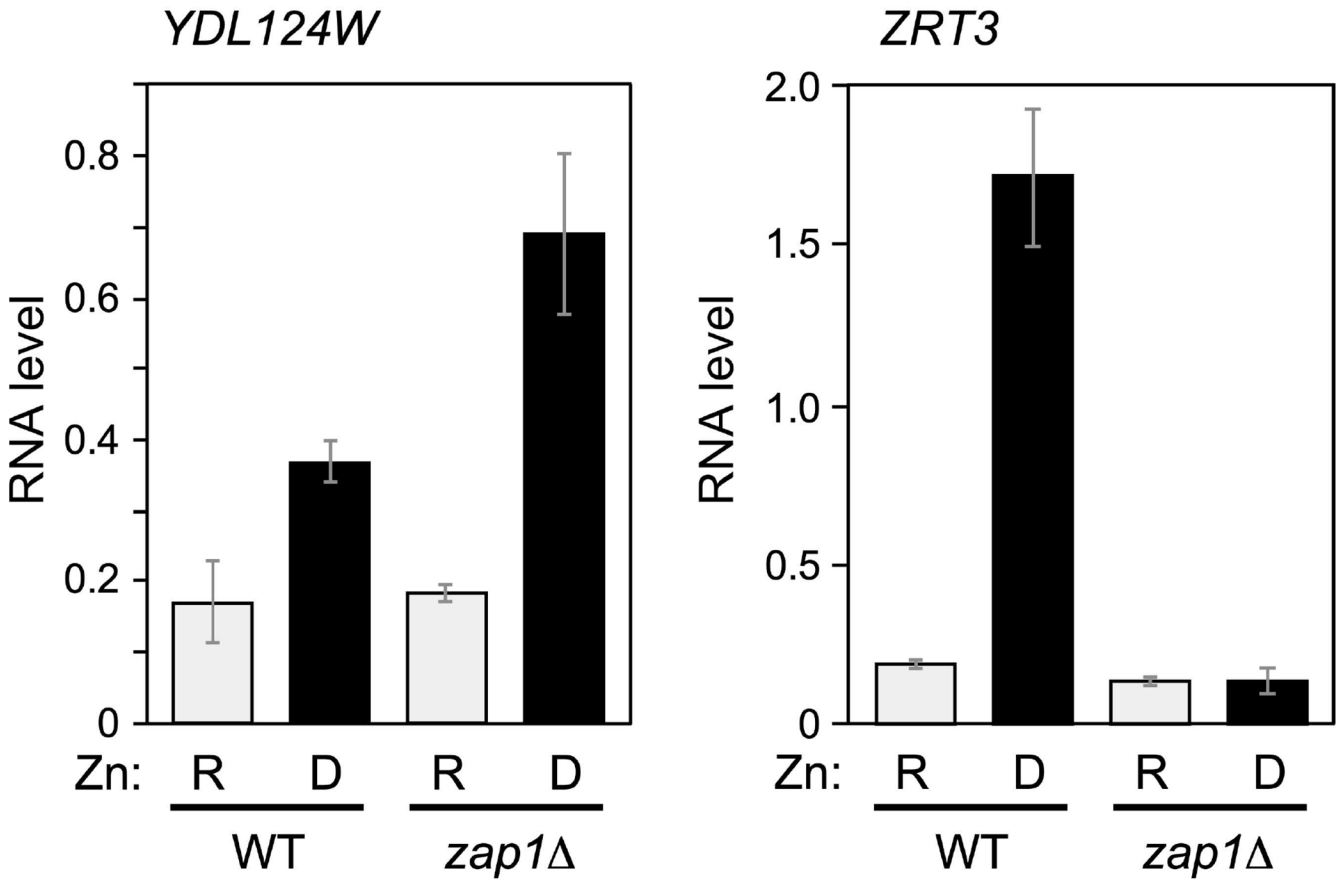

Figure 6. *YDL124W*, the gene adjacent and divergently transcribed from *HNT1* is induced by zinc deficiency but is Zap1-independent.

Wild-type (BY4743) and *zap1Δ* (BY4743 *zap1Δ::KanMX*) mutant cells were grown in LZM + 100 μM $ZnCl_2$ (zinc-replete, R) and LZM + 1 μM $ZnCl_2$ (zinc-deficient, D) media prior to quantitative RT-PCR analysis of *YDL124W* and *ZRT3* RNA abundance. Their abundance was normalized to the average abundance of three control transcripts (*TAF10, ACT1*, and *CMD1*) and plotted as the average of three biological replicates and the error bars denote ± 1 S.D.

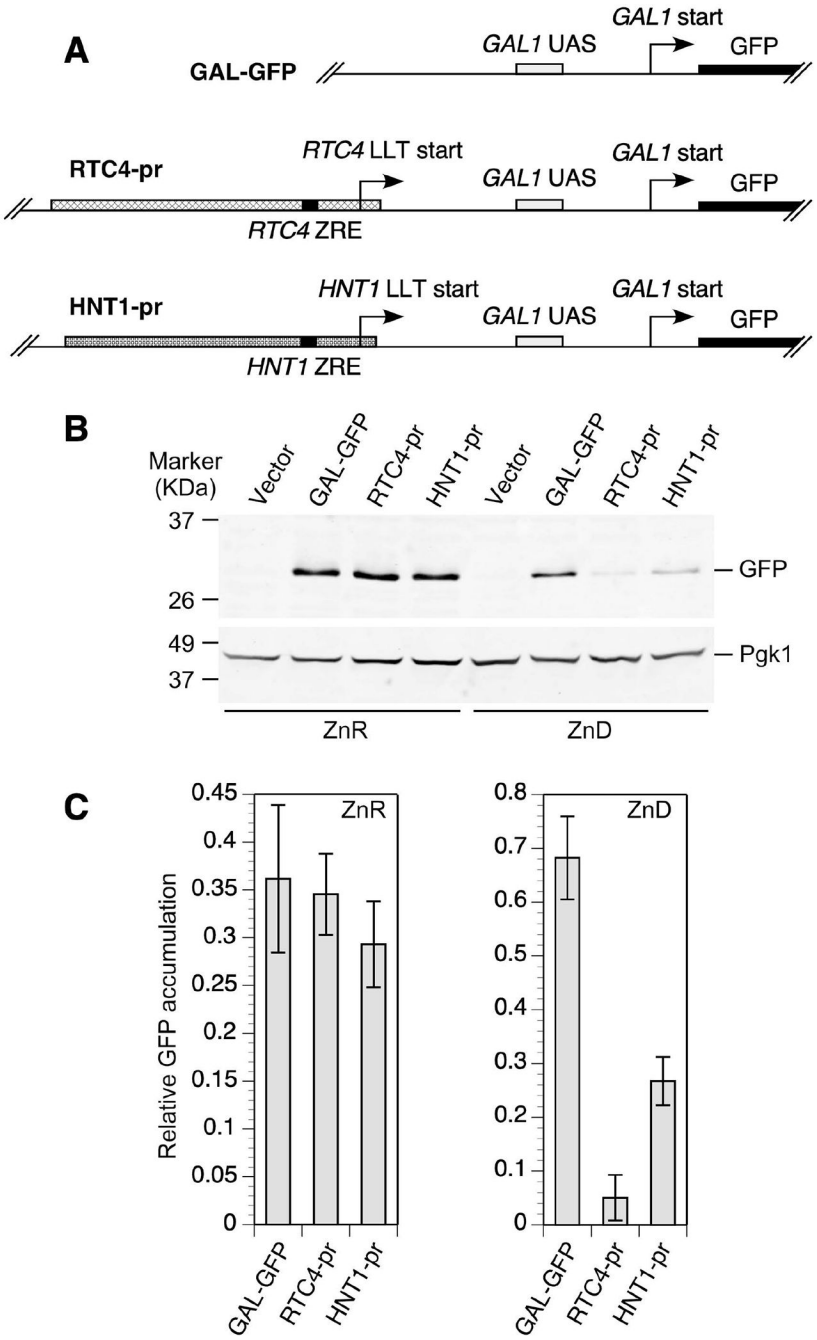

Figure 7. The Zap1-dependent distal promoter driving *HNT1* LLT production can repress a downstream proximal promoter when activated by zinc deficiency.

A) Diagram of the plasmid constructs used. The distal *RTC4* and *HNT1* promoter regions driving their respective LLT RNAs were inserted upstream of the *GAL1* promoter (UAS, upstream activation sequence) and GFP open reading frame. Wild-type (BY4743) cells transformed with the vector pRS316-GAL1, pGAL-GFP (control, *GAL1* promoter alone driving GFP), pRTC4-pr, or pHNT1-pr were grown in LZM + 100 μM $ZnCl_2$ (zinc-replete, R) and LZM + 1 μM $ZnCl_2$ (zinc-deficient, D) media prior to immunoblot analysis using anti-GFP antibody. Shown is one representative blot (panel B) and the average of three

biological replicates is plotted with error bars denoting ± 1 S.D (panel C). The fraction of intensity of each band relative to the total intensity of the three bands in each grouping is plotted. P-values were less than 0.001 for when comparing the zinc-deficient samples to their control; no statistically significant differences were observed among the zinc-replete samples.

Table 1.

Conservation of ZRE-like sequences in the *HNT1* promoters of other *Saccharomyces* species.

	Location[a]	Sequence[b]	p-value[c]
Consensus:	–	ACCTTNAAGGT	–
ZRT1 ZRE1	–	ACCTTCAAGGT	1.0×10^{-6}
UBI4 ZRE1	–	ACCTCTAGGGT	2.2×10^{-5}
HNT1 ZREs			
S. cerevisiae	268	ACCTTTGAGGC	8.5×10^{-5}
S. mikatae	350	ACCTTTGAGCT	9.6×10^{-5}
S. paradoxus	383	ACCCTTGAGGC	9.9×10^{-5}

[a] Distance in base pairs upstream of the *HNT1* ORF.

[b] Nucleotides matching the consensus are underlined.

[c] p-values were determined using MEME.

Table 2.

Effect of intron deletions and *hnt1Δ* mutation on cell growth.

Strain	% in T_o inoculum	Zinc replete			Zinc deficient		
		% after 15 generations	15G/T_o ratio[a]	p-value[b]	% after 15 generations	15G/T_o ratio[a]	p-value[b]
WT	50.3	49.3 ± 0.3	1.0	NS	49.5 ± 0.2	1.0	NS
*HNT1*Δi	53.6	52.9 ± 0.3	1.0	NS	51.2 ± 0.4	1.0	NS
5xΔi	49.3	49.5 ± 0.2	1.0	NS	56.7 ± 0.5	1.2	0.01
hnt1Δ	54.5	49.1 ± 0.8	0.9	0.03	65.4 ± 0.7	1.2	0.008
tsa1Δ	55.0	29.1 ± 0.4	0.5	0.006	4.2 ± 0.2	0.08	0.0004

[a] The ratios of percentage after 15 generations of growth divided by the percentage at T_O are shown.

[b] NS = Not significant.